

Simulation of Natural Convection Flow in an Inclined open Cavity using Lattice Boltzmann Method

H. Sajjadi, M. Gorji, G.H.R. Kefayati, D. D. Ganji, M. Shayan nia

Abstract—In this paper effects of inclination angle on natural convection flow in an open cavity has been analyzed with Lattice Boltzmann Method (LBM). The angle of inclination varied from $\theta = -45^\circ$ to 45° with 15° intervals. Study has been conducted for Rayleigh numbers (Ra) 10^4 to 10^6 . The comparisons show that the average Nusselt number increases with growth of Rayleigh number and the average Nusselt number increase as inclination angles increase at $Ra=10^4$. At $Ra=10^5$ and $Ra=10^6$ the average Nusselt number enhance as inclination angles varied from $\theta = -45^\circ$ to $\theta = 0^\circ$ and decrease as inclination angles increase in $\theta = 0^\circ$ to $\theta = 45^\circ$.

Keywords—Lattice Boltzmann Method, Inclination angle, Open cavity, Natural convection

I. INTRODUCTION

IN the last decades, there has been rapid progress in developing the method of the Lattice Boltzmann Method for solving a variety of fluid dynamics problems. The main advantage of this approach is the enhancement of numerical stability. In addition, implementation of boundary is easy and convection operator is linear [1,2]. In this work, the method is applied for natural convection in inclined open cavity. Natural convection in open cavity applies for various engineering applications, such as solar thermal receiver, heat convection from extended surfaces in heat exchangers and solar collectors with insulated strips [3]. Several numerical simulations are investigated with different states in open cavities and few investigations were done in simple states of open cavity [4-12]. Few researches were utilized for state of inclination and various aspect ratios for open cavity. For instance, Polat et al. [13] studied laminar natural convection in inclined open shallow cavities at range 0° to 45° with interval 15° . They found that the inclination angle of the heated plate is an important parameter affecting volumetric flow rate and the heat transfer. Also, they [14] investigated conjugate heat transfer in inclined open shallow cavities. They obtained the results of inclination effect that were similar to their pervious investigations. Other investigations were researched in an open cavity numerically such as Aminossadati and Ghasemi [15] studied mixed convection in a horizontal channel with a

discrete heat source in an open cavity. Muftuo glu et al. [16] investigated about optimization of discrete heaters on the vertical wall in an open cavity. Experimental investigations were accomplished about open cavity [17-19]. Effect of conduction long the boundaries of the cavities and radiative heat transfer on the heat transfer were verified by Hinojosa et al. [20] and Nouanegue et al. [21] Stability of flow in an open cavity was performed by Javam et al. [22]. Recently, Mohamad et al. [23] studied natural convection in an open cavity numerically with Lattice Boltzmann Method [LBM]. They investigated the effect of systematic analysis of aspect ratio on the physics of flow and heat transfer. They demonstrated that the increasing aspect ratio for a given Rayleigh number decreases the rate of heat transfer up to the conduction limit. The main aim of the present study is to identify the ability of Lattice Boltzmann method (LBM) for various geometries. Effect of inclination on flow and temperature of natural convection are investigated in an open cavity. So stream functions and distribution on the hot wall for different Rayleigh numbers are displayed.

II. MATHEMATICAL FORMULATION

A. Problem statement

A schematic of the two dimensional system with geometrical and boundary conditions is shown in Fig.1. Constant temperature, T_H that is applied on the wall facing the opening was transferred by natural convection to a fluid circulating through the opening to the ambient or a fluid reservoir at a characteristic temperature $T_C=0$. The horizontal walls are assumed to be insulated, non conducting, and impermeable to mass transfer.

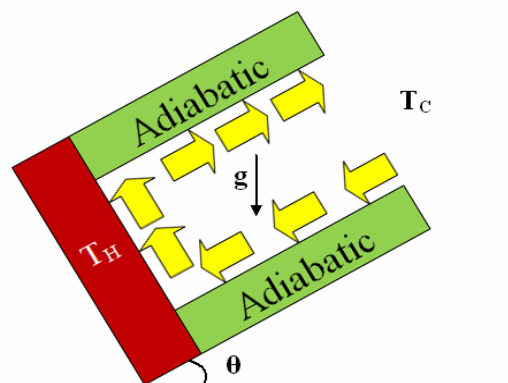


Fig.1 Geometry of the present study

F. A. Department of Mechanical Engineering, Babol Noshirvani University of Technology, Babol, Iran (e-mail: hasansajadi@gmail.com).

S. B. Department of Mechanical Engineering, Babol Noshirvani University of Technology, Babol, Iran (corresponding author to provide phone: 00981113224048; fax: 00981112296582; e-mail: gorji@nit.ac.ir).

T. C. Department of Mechanical Engineering, Babol Noshirvani University of Technology, Babol, Iran (e-mail: ddg_davood@yahoo.com).

F. D. Department of Mechanical Engineering, Babol Noshirvani University of Technology, Babol, Iran (e-mail: rastinreza@yahoo.com).

F. E. Department of Textile Engineering, Guilan University, Rasht, Iran (e-mail: m_shayannia1985@yahoo.com)

B. Lattice Boltzmann Method

For the incompressible flow, if the transport coefficients are independent of the temperature, the energy equation can be decoupled from the mass and momentum equations. For the incompressible thermal problem, He et al. [24] proposed two distribution functions: (1) density distribution function and (2) internal energy density distribution function.

For the flow field:

$$f_i(x+c_i\Delta t, t+\Delta t) - f_i(x, t) = \frac{1}{\tau_v} [f_i(x, t) - f_i^{eq}(x, t)] + \Delta t c_i F \quad (1)$$

For the temperature field:

$$g_i(x+c_i\Delta t, t+\Delta t) - g_i(x, t) = \frac{1}{\tau_c} [g_i(x, t) - g_i^{eq}(x, t)] \quad (2)$$

Standard D2Q9 for flow and D2Q4 for temperature, LBM method is used in this work [2] where the discrete particle velocity vectors defined c_i , Δt denotes lattice time step, τ_v , τ_c is the relaxation time for the flow and temperature fields, respectively, f_i^{eq} , g_i^{eq} are the local equilibrium distribution functions that have an appropriately prescribed functional dependence on the local hydrodynamic properties which are calculated with Eqs. (3) and (4) for flow and temperature fields respectively and F is an external force term.

$$f_i^{eq}(x, t) = \omega_i \rho \left[1 + \frac{c_i u}{c_s^2} + \frac{1}{2} \frac{(c_i u)^2}{c_s^4} - \frac{1}{2} \frac{u u}{c_s^2} \right] \quad (3)$$

$$g_i^{eq} = \omega_i' T \left[1 + \frac{c_i u}{c_s^2} \right] \quad (4)$$

For the 2-D case, applying third-order Gauss-Hermite quadrature leads the following discrete velocities c_i , where $i = 1..8$ and $c_0 = 0$ for D2Q9:

$$c_i = \left(\cos\left(\frac{i-1}{4}\pi\right), \sin\left(\frac{i-1}{4}\pi\right) \right) c \quad (5a)$$

and $i=1..4$ for D2Q4:

$$c_i = \left(\cos\left((i-1)\frac{\pi}{2}\right), \sin\left((i-1)\frac{\pi}{2}\right) \right) c \quad (5b)$$

where $\omega_0=4/9$, $\omega_{1-4}=1/9$, $\omega_{5-8}=1/36$ for density distribution function and $\omega_i'=0.25$ for internal energy density distribution function and (to improve numerical stability, T_m is the mean value of temperature for the calculation of c).

Using a Chapman-Enskog expansion, the Navier-Stokes equations can be recovered with the described model. The kinematic viscosity ν and the thermal diffusivity α are then related to the relaxation times for as follows;

$$\tau_v = 3\mathcal{G} + 0.5 \text{ and } \tau_c = 2\alpha + 0.5$$

In the simulation the Boussinesq approximation is applied to the buoyancy force term. In that case, the external force F appearing in Eq. (1) is given by:

$$F_i = 3\omega_i g_y \beta \Delta T \quad (6)$$

where g_y , β and ΔT are gravitational acceleration, thermal expansion coefficient and temperature difference, respectively.

Finally, the macroscopic variables ρ , u , and T can be calculated using as follows;

$$\text{Flow density: } \rho = \sum_i f_i \quad (7)$$

$$\text{Momentum: } \rho u_j = \sum_i f_i c_{ij} \quad (8)$$

$$\text{Temperature: } \rho RT = \sum_i g_i \quad (9)$$

C. Boundary conditions for flow

Implementation of boundary conditions is very important for the simulation. The unknown distribution functions pointing to the fluid zone at the boundaries nodes must be specified. Concerning the no-slip boundary condition, bounce back boundary condition is used on the solid boundaries [23]. The unknown density distribution functions at the boundary east can be determined by the following conditions:

$$f_{6,n} = f_{6,n-1}, \quad f_{7,n} = f_{7,n-1}, \quad f_{3,n} = f_{3,n-1} \quad (10)$$

D. Boundary conditions for Temperature

The north and south of the boundaries are adiabatic then bounce back boundary condition is used on them. Temperatures at the west and east wall are known. The unknown internal energy distribution functions at the boundary east can be determined by the following conditions:

If $u < 0$ then:

$$g_{3,n} = 0 - g_{1,n} \quad (11a)$$

If $u > 0$ then:

$$g_{3,n} = g_{3,n-1} \quad (11b)$$

E. Lattice Boltzmann method for inclined cavity

It was assumed that cavity is fixed and just force term changed by inclination angles. So all of previous conditions were stabled except the force term that was changed by the following conditions:

$$\text{X direction: } F_i = 3\alpha (g_y \sin\theta) \beta \Delta T \quad (12a)$$

$$\text{Y direction: } F_i = 3\alpha (g_y \cos\theta) \beta \Delta T \quad (12b)$$

III. RESULTS AND DISCUSSION

A. Validation

The open cavity were carried out at different Rayleigh numbers of 10^4 , 10^5 , and 10^6 , with different inclination angles

from $\theta=-45^\circ$ to 45° . The LBM scheme was utilized for obtaining the numerical simulations. Accuracy of present investigation compared with those of studies that were performed by LBM [23] and FVM [7]. So average Nusselt number at hot wall obtained and displayed a good agreement with previous studies (Table.1). Further, the isotherms and streamlines for both methods gave similar results. This comparisons were studied for $\theta=0^\circ$ at $Pr=0.71$.

TABLE I
AVERAGE NUSSLETT NUMBER COMPARISON PREDICTED BY DIFFEREN METHODS

Ra	Present (LBM)	Mohammad (LBM) [23]	Mohammad (FVM) [7]
10^4	3.319	3.377	3.264
10^5	7.391	7.323	7.261
10^6	14.404	14.380	14.076

B. Effect of Rayleigh number on the streamline and isotherm

Fig.2 shows the contour maps for the streamlines and isotherms for various Rayleigh numbers .They demonstrate the streamline and isotherms move upper of open cavity with increase of Rayleigh number. This result obtains because of the growth of buoyancy force. On the other hand isotherms close in walls with increase of Rayleigh number that it causes boundary layer thickness of the hot wall decrease. Therefore an increment in Nusselt number is taking taken place as demonstrated in Fig.3. Also, enhancement of Rayleigh number causes lower portion of open cavity almost to be isothermal. Figs.4-6 illustrate the horizontal velocity of flow at $x=0.5$ for different inclination angles at various Rayleigh numbers. They display that increment of Rayleigh number and buoyancy force accordingly causes the horizontal velocity to increase. Figs.7-9 disclose distribution of temperature at $y=0.5$ for different inclination angles at various Rayleigh numbers. They obviously demonstrated gradient of temperature on hot wall increase with enhancement of Rayleigh number.

C. Effect of inclination angles on the streamline and isotherm

Figs.10-12 shows the contour maps for the streamlines for different inclination angles at various Rayleigh numbers. They show the flow penetrates into the cavity from the lower portion of the opening and leaves from the upper portion of the opening of the cavity clockwise at $\theta=0^\circ$.When inclination angles change from $\theta=0^\circ$ to $\theta=-45^\circ$, develop a recirculation at the near of hot wall clockwise. As inclination angles increase from $\theta=0^\circ$ to $\theta=45^\circ$ for $Ra=10^4$ and 10^5 the streamlines move upper of open cavity but however the strength of buoyancy force is not enough to form recirculation bottom of the open cavity. But at $Ra=10^6$ increase in inclination angles from $\theta=0^\circ$ to $\theta=45^\circ$ causes a weak recirculation to produce at bottom of the open cavity counterclockwise. Figs.13-15 shows the isotherms for different inclination angles at various Rayleigh numbers. When inclination angles enhance from $\theta=0^\circ$ to $\theta=45^\circ$ and change from $\theta=0^\circ$ to $\theta=-45^\circ$ at various Rayleigh

numbers the isotherms recede from the hot wall and gradient of temperature decrease that it causes heat transfer wane accordingly. Figs.4-6 display horizontal velocity increase with increment of inclination angles from $\theta=-45^\circ$ to $\theta=45^\circ$. Production of recirculation in open cavity at $\theta=0^\circ$ to $\theta=-45$ is main result of horizontal velocity decline. Figs.7-9 illustrate gradient of temperature enhance when inclination angles increase from $\theta=-45^\circ$ to $\theta=45$.

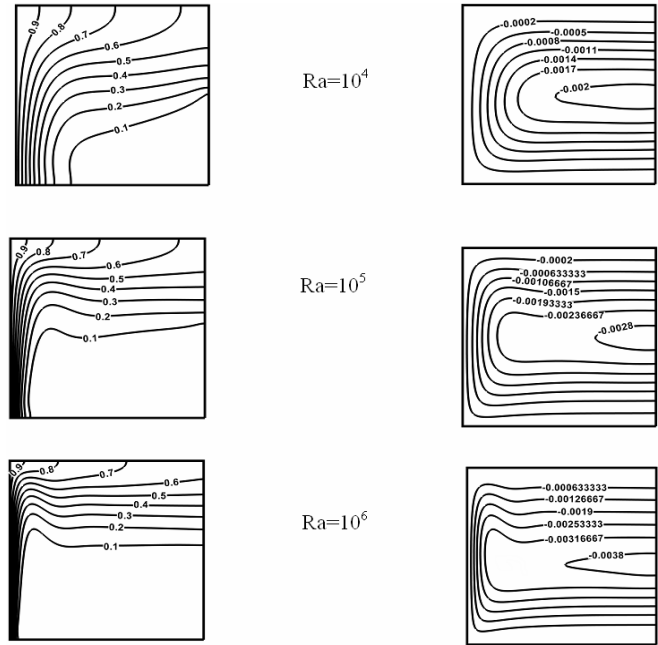


Fig. 2 Comparison of the streamlines and isotherms at $\theta = 0^\circ$ for $Ra= 10^4, 10^5, 10^6$.

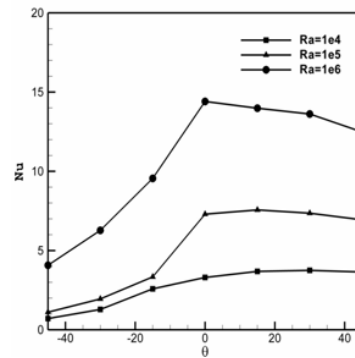


Fig. 3 Average Nusselt number for various inclination angles and different Ra

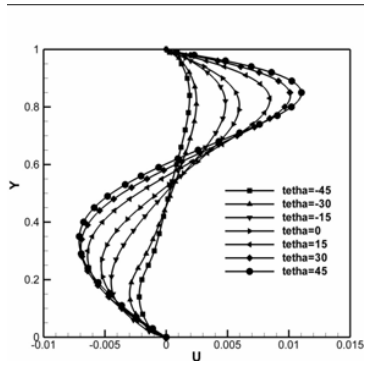


Fig. 4 velocity in midel of cavity for Ra=10⁴

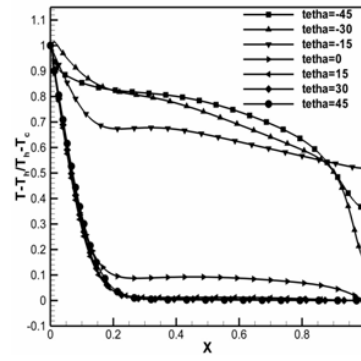


Fig. 8 Temperture in midel of cavity for Ra=10⁵

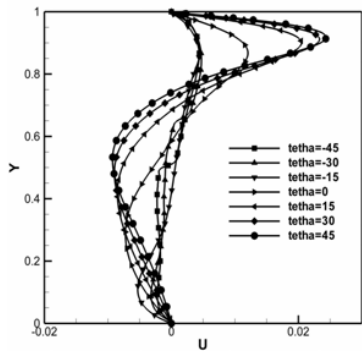


Fig. 5 velocity in midel of cavity for Ra=10⁵

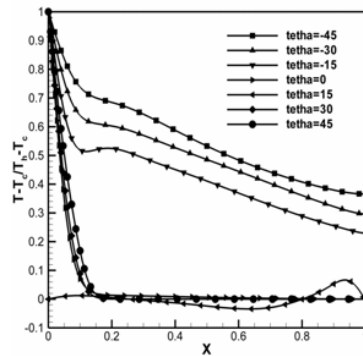


Fig. 9 Temperture in midel of cavity for Ra=10⁶

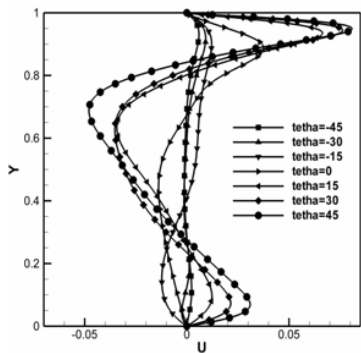


Fig. 6 velocity in midel of cavity for Ra=10⁶

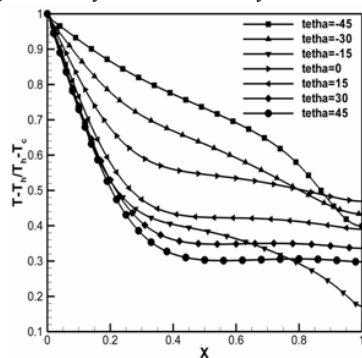


Fig.7 Temperture in midel of cavity for Ra=10⁴

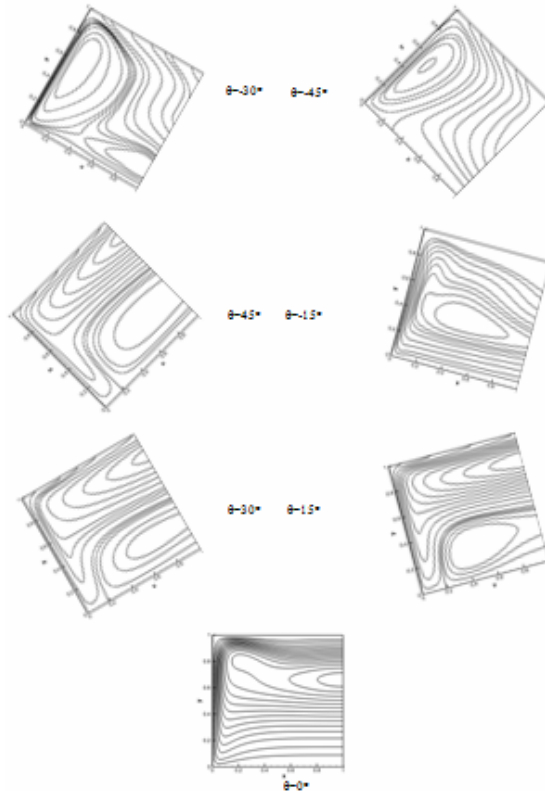


Fig.10 Comparison of the streamlines at Ra=10⁶ for various inclination angles

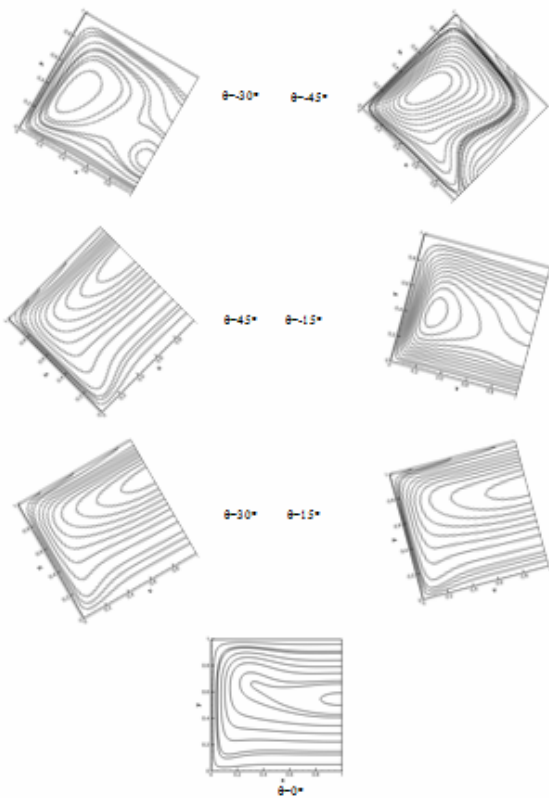


Fig. 11 Comparison of the streamlines at $Ra=10^5$ for various inclination angles

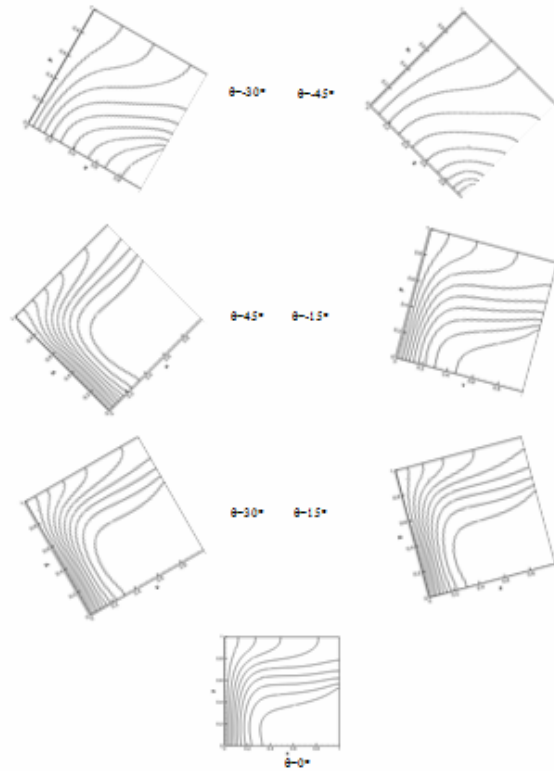


Fig. 13 Comparison of the isotherms at $Ra=10^4$ for various inclination angles

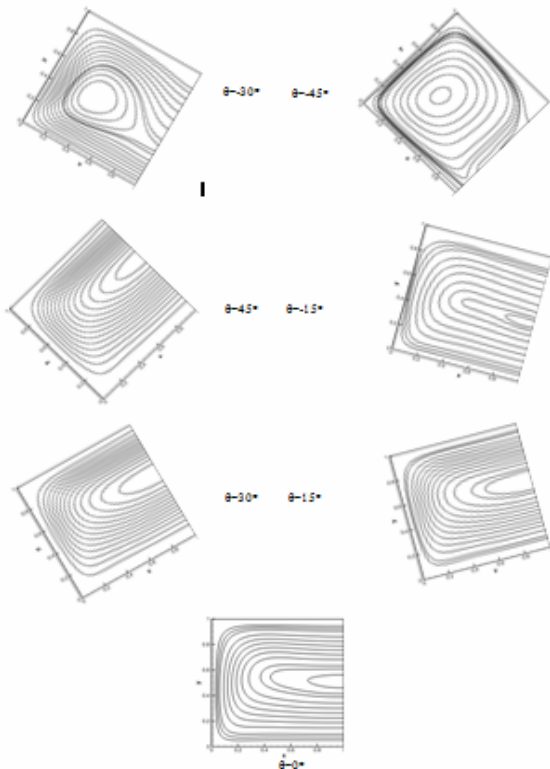


Fig. 12 Comparison of the streamlines at $Ra=10^4$ for various inclination angles

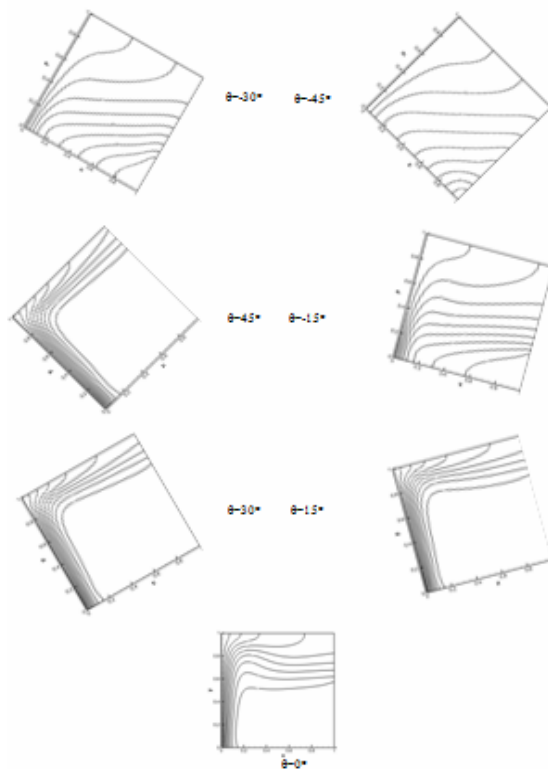


Fig. 14 Comparison of the isotherms at $Ra=10^5$ for various inclination angles

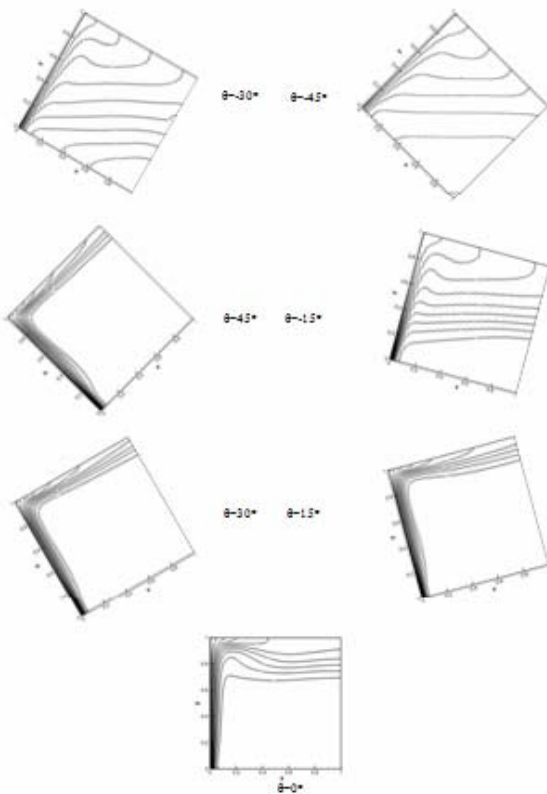


Fig. 15 Comparison of the isotherms at $Ra=10^6$ for various inclination angles

D. Effect of inclination angles on Nusselt number

Fig.3 illustrates the influence of the Rayleigh number and the inclination angles on the average Nusselt number along the heated surface (NU_{avg}). It shows that the NU_{avg} increases with growth of Rayleigh number which it is due to increase in convection heat transfer by Rayleigh number. It displays decrease in value of NU_{avg} at various inclination angles for high Rayleigh numbers of $10^5, 10^6$. On the other hand Figs.10,11 show a weak flow in bottom of inclined open cavity that is opposite direction of main flow, counterclockwise and causes to decrease convection heat transfer at inclined open cavity for $Ra=10^5, 10^6$. Fig.16 shows the variation of local Nusselt number along the hot wall at different inclination angles and various Ra. It displays local Nusselt number along the hot wall at different inclination angles for equal Ra has similar process. On the other hand NU_{max} on hot wall decreases with increase in inclination angles.

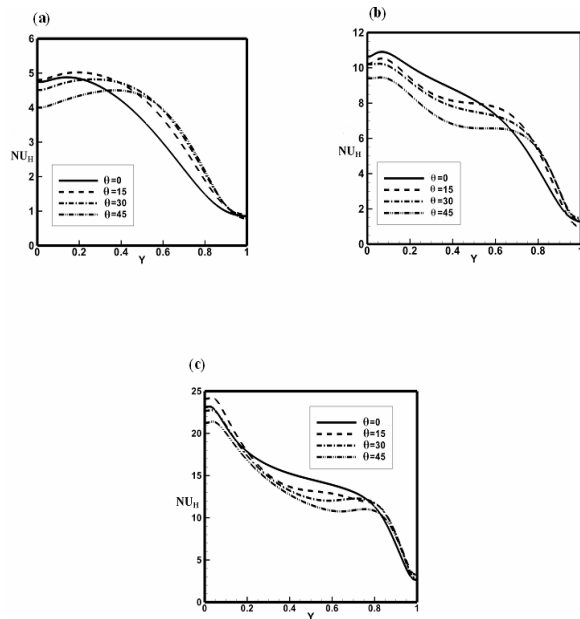


Fig. 16 Nusselt number distributions on the hot wall at different inclination angles for (a) $Ra=10^4$ (b) $Ra=10^5$ (c) $Ra=10^6$

IV. CONCLUSIONS

This study has been carried out for the pertinent parameters in the following ranges: the Rayleigh number of fluid, $Ra=10^4-10^6$, and inclination angles (θ) of the cavity between -45° and 45° with interval 15° . The results of LBM were validated with previous numerical investigations and it illustrated a good agreement. This investigation demonstrated the ability of LBM for simulation of different geometries. The comparisons show that the average Nusselt number increases with growth of Rayleigh number. Inclination angles cause to produce another circulation on bottom of open cavity oppositely with main circulation at high Rayleigh numbers. The average Nusselt number decreases as inclination angles increase at high Rayleigh numbers.

REFERENCES

- [1] A. D'Orazio, M. Corcione, G. P. Celata, Application to natural convection enclosed flows of a Lattice Boltzmann BGK model coupled with a general purpose thermal boundary condition, *Int. J. Thermal Sciences*, vol. 43, pp. 575-586, 2004.
- [2] A.A. Mohamad, *Applied Lattice Boltzmann Method for Transport Phenomena, Momentum, Heat Mass Transfer*, Sure, Calgary, 2007.
- [3] I. Sazia, A.A. Mohamad, Suppressing free convection from a flat plate with poor conductor ribs, *Int. J. Heat Mass Transfer*, vol. 42, pp. 2041-2051, 1999.
- [4] P. Le Quere, J.A.C. Humphrey, F.S. Sherman, Numerical calculation of thermally driven two-dimensional unsteady laminar flow in cavities of rectangular cross section, *Numer. Heat Transfer Part A*, vol. 4, pp. 249-283, 1981.
- [5] F. Penot, Numerical calculation of two-dimensional natural convection in isothermal cavities, *Numerical Heat Transfer Part A*, vol. 5, pp. 421-437, 1982.

- [6] Y.L. Chan and C.L. Tien, A numerical study of two-dimensional natural convection in square open cavities, *Numer. Heat Transfer Part A*, vol. 8, pp. 65–80, 1985.
- [7] A.A. Mohamad, Natural convection in open cavities and slots, *Numer. Heat Transfer Part A*, vol. 27, pp. 705–716, 1995.
- [8] D. Angirasa, M. J. B. M. Pourquie, F. T. M. Nieuwstadt, Numerical study of transient and steady laminar buoyancy-driven flows and heat transfer in a square open cavity, *Numer. Heat Transfer Part A*, vol. 22, pp. 223 – 239, 1992.
- [9] T. H. Hsu and K. Y. Hong, Natural Convection of Micropolar Fluids in an Open Cavity, *Numer. Heat Transfer Part A*, vol. 50, pp. 281 – 300, 2006.
- [10] D. Angirasa, J. G. M. Eggels, F. T. M. Nieuwstadt, Numerical simulation of transient natural convection from an isothermal cavity open on a side, *Numer. Heat Transfer Part A*, vol. 28, pp. 755 – 767, 1995.
- [11] J. F. Hinojosa, C. A. Estrada, R. E. Cabanillas, G. Alvarez, Numerical Study of Transient and Steady-State Natural Convection and Surface Thermal Radiation in a Horizontal Square Open Cavity, *Numer. Heat Transfer Part A*, vol. 28, pp. 179 – 196, 2005.
- [12] M. Miyamoto, T.H. Huehn, J. Goldstein, Y. Katoh, Two dimensional laminar natural convection heat transfer from a fully or partially open square cavity, *Numer. Heat Transfer Part A*, vol. 15, pp. 411–430, 1989.
- [13] O. Polat and E. Bilgen, Laminar natural convection in inclined open shallow cavities, *Int. J. Thermal Sciences*, vol. 41, pp. 360–368, 2002.
- [14] O. Polat and E. Bilgen, Conjugate heat transfer in inclined open shallow cavities, *Int. J. Heat Mass Transfer*, vol. 46, pp. 1563–1573, 2003.
- [15] S.M. Aminossadati and B. Ghasemi, A numerical study of mix convection in a horizontal channel with a discrete heat source in an open cavity, *Eur. J. Mech. B/Fluids*, vol. 28, pp. 590-598, 2009.
- [16] A. Muftuo glu and E. Bilgen, Natural convection in an open square cavity with discrete heaters at their optimized positions, *Int. J. Thermal Sciences*, vol. 47, pp. 369–377, 2008.
- [17] Y.L. Chan and C.L. Tien, Laminar natural convection in shallow open cavities, *Int. J. Heat Transfer*, vol. 108, pp. 305–309, 1986.
- [18] E. Bilgen, Passive solar massive wall systems with fins attached on the heated wall and without glazing, *J. Sol. Energ. Eng.*, vol. 122, pp. 30–34, 2000.
- [19] S.S.Cha and K.J. Choi, An interferometric investigation of open cavity natural convection heat transfer, *Exp. Heat Transfer*, vol. 2, pp. 27–40, 1989.
- [20] J.F. Hinojosa, R.E. Cabanillas, G. Alvarez, C.E. Estrada, Nusslet number for the natural convection and surface thermal radiation in a square tilted open cavity, *Int. Comm. Heat Mass Transfer*, vol. 32, pp. 1184–1192, 2005.
- [21] N. Nouanegue, A. Muftuo glu, E. Bilgen, Conjugate heat transfer by natural convection, conduction and radiation in open cavities, *Int. J. Heat Mass Transfer*, pp. 779-788, 2008.
- [22] A. Javam and S.W. Armfield, Stability and transition of stratified natural convection flow in open cavities, *J. Fluid Mech.*, vol. 44, pp. 285–303, 2001.
- [23] A.A. Mohamad, M. El-Ganaoui, R. Bennacer, Lattice Boltzmann simulation of natural convection in an open ended cavity, *Int. J. Thermal Sciences*, vol. 48, pp. 1870–1875, 2009.
- [24] X. He, S. Chen and G.D. Doolen, A novel thermal model for the lattice Boltzmann method in incompressible limit, *J. Comput. Phys.*, vol. 146, pp. 282–300, 1998.